Multidimensional, Non-Isothermal, Dynamic Modelling Of Planar Solid Oxide Fuel Cells

K. Tseronis[a], I. Kookos[b], C. Theodoropoulos[a*]

[a]School of Chemical Engineering and Analytical Science, University of Manchester, Manchester M60 1QD, UK

[b]Department of Chemical Engineering, University of Patras, 26500 Patras, Greece

A multidimensional, multicomponent, non-isothermal, dynamic model that simulates the mass and energy transport as well as the electrochemical phenomena taking place in a single planar solid oxide fuel cell (SOFC) is presented. It is used for predicting species composition profiles, temperature profiles and polarisation curves in order to analyse the effect of various design parameters and operating conditions on SOFC performance. Moreover, the dynamic response of the SOFC current density for step changes of various system inputs is investigated. The model is implemented in a two-dimensional computational domain however the underlying theory is independent of the geometry used. SOFCs operate more efficiently at high operating temperatures and pressures. The computed dynamic response of the current density is found to be in the same range with results from the literature.

1. Introduction

Solid oxide fuel cells (SOFCs) receive considerable interest nowadays because of their potential for achieving greater electrical efficiency than that obtained by conventional heat engines or by other types of low temperature fuel cells (Kordesch & Gunter, 1996, Larminie & Dicks, 2003). The objective of this work is to develop a detailed mathematical model that will be capable to describe the fundamental electrochemical and transport phenomena occurring in the SOFC. Such phenomena are very difficult to measure experimentally, especially at the high operating temperatures that characterise the SOFCs operation. Mathematical modelling can offer an alternative approach for the detailed study of the SOFC behaviour reducing the number of experiments required. The model presented here can predict the effects of different operating and design parameters on the performance of SOFCs including the system dynamics. The effect of various operating parameters on the SOFC performance is investigated through the polarisation curves generated by the model. Finally, dynamic responses of the SOFC current density to step responses of the SOFC operating voltage and fuel and air inlet temperatures are computed. Knowledge and understanding of SOFC dynamics can be very important for the selection of appropriate control strategies and for efficient and robust controller design.

---

[*] Corresponding author: k.theodoropoulos@manchester.ac.uk

2. SOFC Electrochemistry

A typical SOFC, schematically depicted in Fig.1, consists of two electrodes, the anode and the cathode with the electrolyte laying between them. The electrolyte plays the role of a separator for the fuel and the air, which otherwise would react through direct combustion. The electrochemical reactions that take place at the SOFC electrodes are as follows: $ANODE: H_2 + O^{2-} \rightarrow H_2O + 2e^- \qquad CATHODE: 1/2\,O_2 + 2e^- \rightarrow O_2^-$.
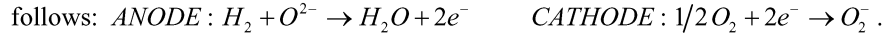
Based on these half-cell reactions, the overall reaction occurring can be written as:

$$H_2 + 1/2\,O_2 \leftrightarrow H_2O \; ; \; \Delta H^0_{1073K} = -250 kJ \; mol^{-1} \tag{1}$$
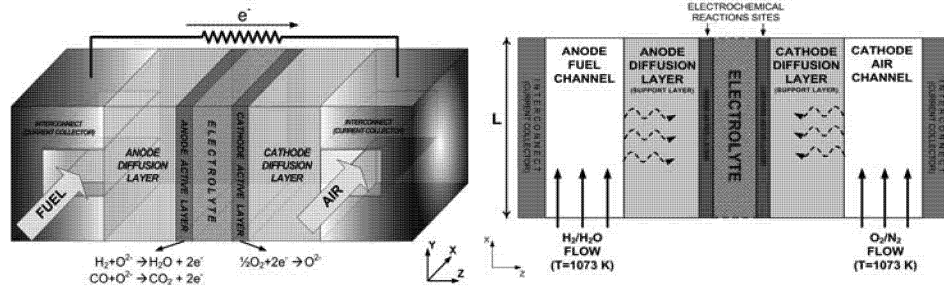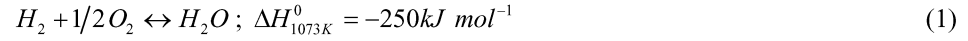

Fig.1 Schematic of the basic operation principles of a planar SOFC & the computational domain of the model (X-Z cross section).

3. SOFC Model

The SOFC model presented here is used to simulate the mass and energy transport as well as the electrochemical effects that take place in the fuel and air channels, the porous electrodes, the electrolyte and the interconnects of a single cell of a planar SOFC stack using the finite-element (FE) method exploited by the software COMSOL Multiphysics. Fuel composition is comprised of H_2 and H_2O at the anode side and of O_2 and N_2 at the cathode side, where air is used as oxidant.

3.1 Model description and computational domain

In the fuel and air channels as well as in the porous electrodes of the SOFC multicomponent mass transfer by convection and diffusion takes place. The thin catalyst layers where fuel and oxidant are electrochemically converted into electrical work, heat and water vapour will be treated as interface boundaries in the current model (rather than finite regions). The processes that take place at these interfaces are the electrochemical reactions and the generation of heat from these reactions. In Fig.1 the 2-D computational domain used for the SOFC model is depicted. This domain represents a X-Z cross-section through a planar SOFC and is divided into various subdomains. The dimension along the length of the fuel channel (X-dimension) and the one normal to the reactive surface at the electrode-electrolyte interface (Z-dimension) are considered. Symmetry was assumed at the interconnect boundaries in the Z-direction.

3.2 Multicomponent mass transport

The differential form of the continuity equation for component i , if ideal gas behaviour is assumed, can be written as follows (Welty et al., 2000):

$$\frac{\varepsilon}{RT}\frac{\partial p_i}{\partial t} = -\nabla \cdot N_i \qquad (2)$$

where ε is the porosity (equal to unity for the gas phase) and $\mathbf{N}_i$ the total molecular flux of species i. The Stefan-Maxwell model will be used for the simulation of the fuel and the air channel and its mathematical formulation is described in detail in (Welty et al., 2000). For the simulation of the porous electrodes at the anode and the cathode, the Dusty Gas model (Mason & Malinauskas, 1983), which is considered the most accurate of the existing mass transfer models in porous media (Suwanwarangkul, 2003; Tseronis et al, 2007), will be used. Its mathematical formulation can be found in (Mason & Malinauskas, 1983; Tseronis et al., 2006, Tseronis et al, 2007):

3.3 Energy transport

The energy transport equation is solved in all the subdomains of the computational domain. The dominant phenomena are heat conduction and convection. The governing equation which describes these phenomena is:

$$\rho C_p \frac{\partial T}{\partial t} = -\nabla \cdot \left(-k\nabla T\right) - \rho C_p \mathbf{V} \cdot \nabla T + Q_h \qquad (3)$$

where ρ is the total density of the gas, C_p is the heat capacity of the gas or the conducting material, k the thermal conductivity, $\mathbf{V}$ the velocity vector and $Q_h = \Delta H \cdot r_e \cdot \dfrac{1}{w_E}$ represents the thermal source. For the electrolyte subdomain is

$\Delta H^0_{1073K} = -250 kJ\ mol^{-1}$ w_E= is the width of the electrolyte=0.5mm and $r_e = \dfrac{I_c}{2F}$ is the electrochemical reaction rate, I_c being the current density and F the Faraday constant.

3.4 Electrochemical model

The difference between the thermodynamic potentials of the electrode reactions determines the open circuit voltage (OCV) of the SOFC, which is the theoretical voltage that can be achieved under specific operating conditions. However, the operating voltage of a SOFC is usually much lower than the OCV, due to the overpotentials that occur when current is drawn and when the electrochemical reactions take place. The operating voltage V_c of a SOFC is given by the following equation (Aguiar et al., 2004; Larminie & Dicks, 2003):

$$V_C = V_{Nernst} - \left(\eta^A_{conc} + \eta^C_{conc} + \eta^A_{act} + \eta^C_{act} + \eta_{ohm}\right) \qquad (4)$$

The activation overpotential (η_{act}) is represented by the Butler-Volmer equation:

$$I_C = I_0\left[\exp\left(a\ \frac{n_e F}{RT}\eta_{act}\right) - \exp\left(-\left(1-a\right)\frac{n_e F}{RT}\eta_{act}\right)\right] \qquad (5)$$

where a is the transfer coefficient, n_e the number of electrons transferred in the electrochemical half-cell reaction and I_0 the exchange current density for the anode/cathode electrode. The concentration overpotential (η_{conc}) results from the failure to transport sufficient reactant through the porous electrodes to the reaction sites at the

electrode/electrolyte interface in order to satisfy the demand for fuel or air. It is given, in terms of partial pressures at the reaction sites (i.e at the triple phase boundary -TPB) and at the bulk of the fuel channel (Aguiar et al., 2004):

$$\eta_{conc}^A = -\frac{RT}{n_e F}\ln\left(\frac{p_{H_2}^{bulk}\, p_{H_2O}^{TPB}}{p_{H_2}^{TPB}\, p_{H_2O}^{bulk}}\right) \text{ and } \eta_{conc}^C = -\frac{RT}{n_e F}\ln\left(\frac{p_{O_2}^{bulk}}{p_{O_2}^{TPB}}\right) \tag{6}$$

The ohmic overpotential (η_{ohm}) is caused by the resistance to the conduction of ions through the electrolyte and to the conduction of electrons through the electrodes (Aguiar et al., 2004): $\eta_{ohm} = I_C R_{ohm}$, where R_{ohm} is the internal ohmic resistance of the SOFC which consists of electronic and ionic resistances.

4. Results and Discussion

For the solution of the system of coupled algebraic/partial differential equations (PDEs) the (FE) method-based PDE solver COMSOL Multiphysics 3.2a is used. For the inversion of the Jacobian matrices at each iteration of the nonlinear solver, the direct linear solver UMFPACK for non symmetric systems was used.

4.1 Steady-state results
In Fig.2a the H_2 and O_2 molar fractions at the anode fuel channel and at the cathode air channel are illustrated respectively. As hydrogen and oxygen flow in the fuel and air channel respectively they diffuse through the porous electrodes where they are being consumed at the electrode/electrolyte interfaces. Fig.2b shows the temperature distribution at the SOFC for inlet temperatures at the anode fuel channel T_{FC}=1073K and at the cathode air channel T_{AC}=1023K. As it can be seen the heat of the gas streams is transferred along the X-direction via convection by the gas flow and along the Z-direction mainly by conduction. Heat generation takes place at the boundaries of the anode and the cathode porous electrodes with the electrolyte due to the exothermic electrochemical reactions. At the left and right ends of the domain symmetry conditions apply, since the cell is considered to be in the middle of a SOFC stack.
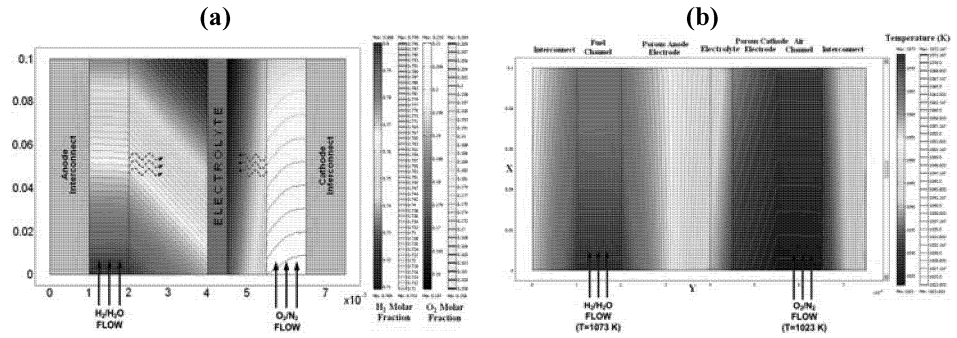

Fig.2(a) H_2 and O_2 molar fraction distributions & (b) temperature distribution for binary gas mixtures of H_2-H_2O ($y_{H_2}^0 = 0.8$) and O_2-N_2 ($y_{O_2}^0 = 0.21$) and for fuel and air channel inlet temperatures T_{FC}=1073K and T_{AC}=1023K.

The effect of the inlet temperature at the fuel and air channels, T_{FC} and T_{AC} as well as the effect of operating pressure on the SOFC performance are illustrated in Fig.3. The total SOFC performance, measured by the maximum power density, P_c, as well as the limiting current density (I_c corresponding to V_c=0) both increase with increasing temperature. A slight decrease in the OCV, (V_c corresponding to I_c=0) can be observed as the temperature expectedly increases. From the polarisation curves shown in Fig. 3b it can be seen that by increasing the operating pressure, the SOFC overall performance will also increase. As pressure decreases the OCV decreases accordingly which is also expected. Furthermore, with increasing operating pressure the limiting current density increases.
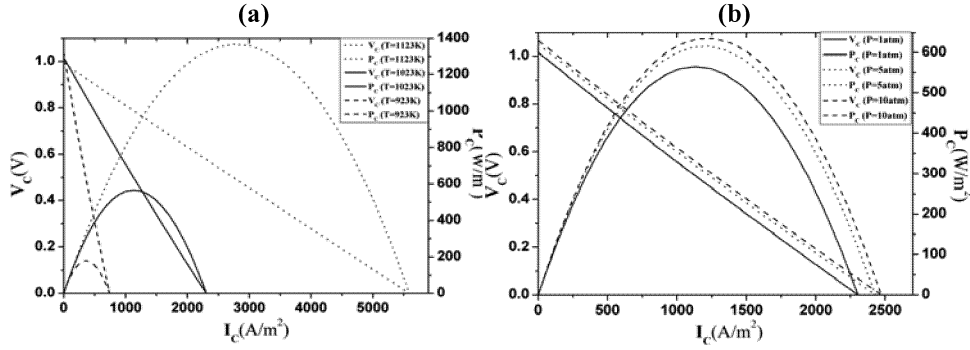
(a)   **(b)**

Fig.3 (a) Operating voltage V_C and power density P_C as functions of current density I_C for different fuel and air channel inlet temperatures T_{FC} and T_{AC} (1123K - 1023K - 973K) as well as (b) for different SOFC operating pressures P (1atm - 5atm - 10atm).

4.2 Dynamic results

Fig.4a shows the open loop response of the average current density I_C of the SOFC when the operating voltage V_C undergoes step changes from 0.65 V to 0.55 V and to 0.45 V. Furthermore, the open loop response of the average current density I_C of the SOFC when the inlet temperatures of the fuel and air channel undergo a step change from 1023 K to 973 K and to 1073 K is depicted in Fig.4b. A larger transient response time is demonstrated in the second case, which can be attributed to the slower dynamics of the energy transport phenomena when compared to the mass transport phenomena, which agrees with published SOFC dynamic studies (e.g. Um et al., 2000).
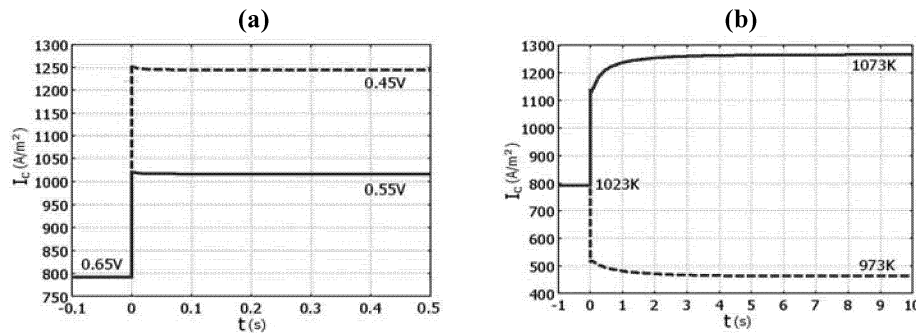
(a)   **(b)**

Fig.4(a) Dynamic current density I_C response to step changes in the operating voltage V_C from 0.65V to 0.55V and 0.45V and (b) to step changes in the inlet temperatures of the fuel and air channel T_{FC} and T_{AC} from 1023 K to 973 K and 1073 K.

5. Conclusions

An anode-supported, single-cell, multidimensional, multicomponent, non-isothermal, dynamic model of the mass and energy transport and of the electrochemical phenomena taking place in the SOFC was presented. Composition and temperature distribution profiles were obtained and it was shown that variation of the inlet temperatures of the fuel and air channels can lead to the formation of temperature gradients in the SOFC. Polarisation curves are also generated to study the effect of temperature and operating pressure on the SOFC performance. Finally, dynamic responses of the average current density to step changes in the operating voltage and the inlet temperatures of the gas streams at the anode and the cathode are computed.

The model provides a better understanding of the physico-chemical phenomena underlying SOFC operation and can lead to designs and operating conditions which will optimise the performance of SOFC systems.

Acknowledgements

References

Aguiar, P., C.S. Adjiman, and N.P. Brandon, 2004, Journal of Power Sources, 138, 1-2.

Kordesch,K. and S. Gunter, 1996, Fuel Cells and their Applications. VCH, New York.

Larminie, J. and A. Dicks, 2003, *Fuel Cell Systems Explained*, Wiley & Sons, New York.

Mason, E.A. and A.P. Malinauskas, 1983, *Gas Transport in Porous Media: The Dusty-Gas Model*. Elsevier, Amsterdam.

Suwanwarangkul, R., E. Croiset, M.W. Fowler, P.L. Douglas, E. Entchev and M.A. Douglas, 2003, Journal of Power Sources, 122, 1.

Tseronis, K., I. Kookos, I., and C. Theodoropoulos, Modelling and Design of Solid Oxide Fuel Cell Systems. Conference Proceedings of the 17th International Congress of Chemical and Process Engineering, Prague.

Tseronis, K., I. Kookos, and C. Theodoropoulos, C., 2007, Journal of Power Sources, *submitted*

Um, S., C.-Y. Wang, and K.S. Chen, 2000, Journal of The Electrochemical Society, 147, 12.

Welty, J.R., C.E. Wicks, R.E. Wilson and G. Rorrer, 2000, *Fundamentals of Momentum, Heat and Mass Transfer*. 4th ed. John Wiley & Sons, New York.